

SOME IMPROVEMENTS UPON ELECTRONIC METAL LOCATORS
OF THE RECEIVER-TRANSMITTER VARIETY

by
Donald Edward Lancaster

A Thesis Presented in Partial Fulfillment
of the Requirements for the Degree
Master of Science in Engineering

ARIZONA STATE UNIVERSITY
May, 1966

SOME IMPROVEMENTS UPON ELECTRONIC METAL LOCATORS
OF THE RECEIVER-TRANSMITTER VARIETY

by
Donald Edward Lancaster
has been approved
May, 1966

APPROVED:

Carl R. Zinner
A. B. Donnelly
E. L. Jordan
Frank B. Thompson

Supervisory Committee

ACCEPTED:

Frank B. Thompson
Department Chairman
(If appropriate, Dean of the College)

W. J. Smith
Dean, Graduate College

TABLE OF CONTENTS

ABSTRACT	ii
INTRODUCTION	1
OPTIMUM GEOMETRY	3
CHOICE OF FREQUENCY	12
RECEIVER SENSITIVITY AND BANDWIDTH	16
SIGNAL PROCESSING TECHNIQUES	18
SYSTEM BLOCK DIAGRAM	22
USE OF INTEGRATED CIRCUITS	24
COMPLETE SCHEMATIC	31
DEMONSTRATION MODEL	35
EXPERIMENTAL RESULTS	44
FURTHER WORK	45
CONCLUSIONS	47
BIBLIOGRAPHY	49

SOME IMPROVEMENTS UPON ELECTRONIC
METAL LOCATORS OF THE
RECEIVER-TRANSMITTER VARIETY

by

Donald Edward Lancaster

ABSTRACT

The present availability of integrated circuits makes possible several substantial improvements upon underground electronic metal locators of the radio frequency receiver-transmitter variety. These include a reduction of the field pattern distortion through reduced circuit sizes, a lower cost, lighter weight, a better mechanical stability, and the ability to use ordinary penlight cells for power.

An analysis of the optimum geometry, antenna parameters, and operating frequency is made and related to geophysical data, taking into account the requirements for a portable instrument. This is followed by an investigation of the receiver sensitivity and transmitted power requirements. Optimum signal processing is considered, concluding that both nonlinear and synchronous techniques are of value in the reduction of unwanted signal returns.

The theoretical design is related to currently available integrated components, evolving in a complete electronic and mechanical design for a portable instrument. A successful model of the circuitry is described along with comparative results.

INTRODUCTION

The present availability of low cost integrated circuitry strongly suggests application of these new components to portable underground metal locators. Of the four basic types of electronic locator,¹ the receiver-transmitter variety has consistently demonstrated the greatest penetration capability when applied to moderate sized objects, but has been limited by its bulk and relatively high circuit cost. Such instruments finds wide use among public utility companies for accurate location of buried pipes and cables, by geophysical prospectors for location and tracing of mineral veins, and by outdoorsmen and electronic experimenters for "treasure hunting" applications.

One of the potential benefits of integrated circuitry applied to this end is the reduction of field pattern distortion caused by the presence of excess metal on conventional designs, as is required in the form of chassis, battery mounts, cabling, and the like. The net effect of such metal is to produce a minimum nonnullable common-mode signal which defines the limit of receiver sensitivity. The design to be described makes use of ordinary penlight cells as a power source. These are considerably lower in cost and more readily available than the specialized batteries normally employed. Another major benefit is the ability to produce a very light weight instrument of sufficient mechanical stability for high sensitivity.

Low cost is certainly an objective in any instrument of this type. The integrated circuits to be described are already far cheaper than their discrete counterparts. Further, the matching and temperature tracking inherent in integrated circuitry allows the use of balanced differential amplifier stages with their simplified biasing and reduced external circuitry requirements.

For these reasons, a design analysis using integrated circuitry was carried out, resulting in a model instrument with features of demonstrative superiority to conventional detectors.

OPTIMUM GEOMETRY

The locator must be both portable and readily transportable if it is to be of practical field value. Limits may be placed upon the maximum allowable dimensions of the design, which may be set at 60 inches long, 20 inches wide, and less than 10 pounds in weight. It is within these limits that the optimum geometry and frequency is to be determined.

Loop antennas are chosen for both a vertical rear transmitting antenna and a horizontal forward receiving antenna, using the orthogonality of the loop null axes to obtain cancellation of the straight-through signal. The use of loops is based upon its previous success in this field and upon the fact that the null axis is broadside to the antenna itself.

For any antenna, the transition zone between the near and far fields is given by the relation²

$$R = \frac{2a^2}{\lambda}$$

where

R = distance to transition zone, meters

a = antenna aperture, meters

λ = wavelength, meters.

The transition zone reaches a maximum at maximum aperture and frequency. For a = 20 inches and a frequency f of 10 MHz, the transition zone occurs only 1.75 centimeters away from the antenna. Thus all loops considered are clearly in the far field.

For any loop antenna, the far field voltage is given by³

$$E_{\phi} = 30 \beta^3 i a \left[\frac{1}{[\beta r]} - \frac{j}{[\beta r]^2} \right] \sin \psi e^{-j\beta r}$$

where

E_{ϕ} = field strength, volts

i = loop current, amperes

a = loop area, meters²

r = radial distance from loop center, meters

ψ = angular deviation from loop null axis

$\beta = 2\pi/\lambda$.

The equation in this form reveals both a real and an inductive term to the induced voltage. At $\beta r = 1$, both field terms are of equal significance. Again taking a frequency of 10 MHz, this occurs at $r = 15.7$ feet. Since this is beyond the intended range of operation, the field equations may be reduced to include only the inductive far field term, and the depth and resolution capabilities may then be based upon mutual inductance calculations.

Figure 1 shows the mathematical model employed.

A small spherical radiator forms the target, buried a distance x directly below the single turn receiving loop. The receiving loop is rotated an angle θ from vertical. In practice, θ would be as near to 90 degrees as mechanically possible. The model assumes a lossless, homogenous medium, which will be related below to actual terrestrial conditions.

The coefficient of coupling k between a single turn loop antenna and a small spherical highly conductive target of diameter D is given by¹⁴

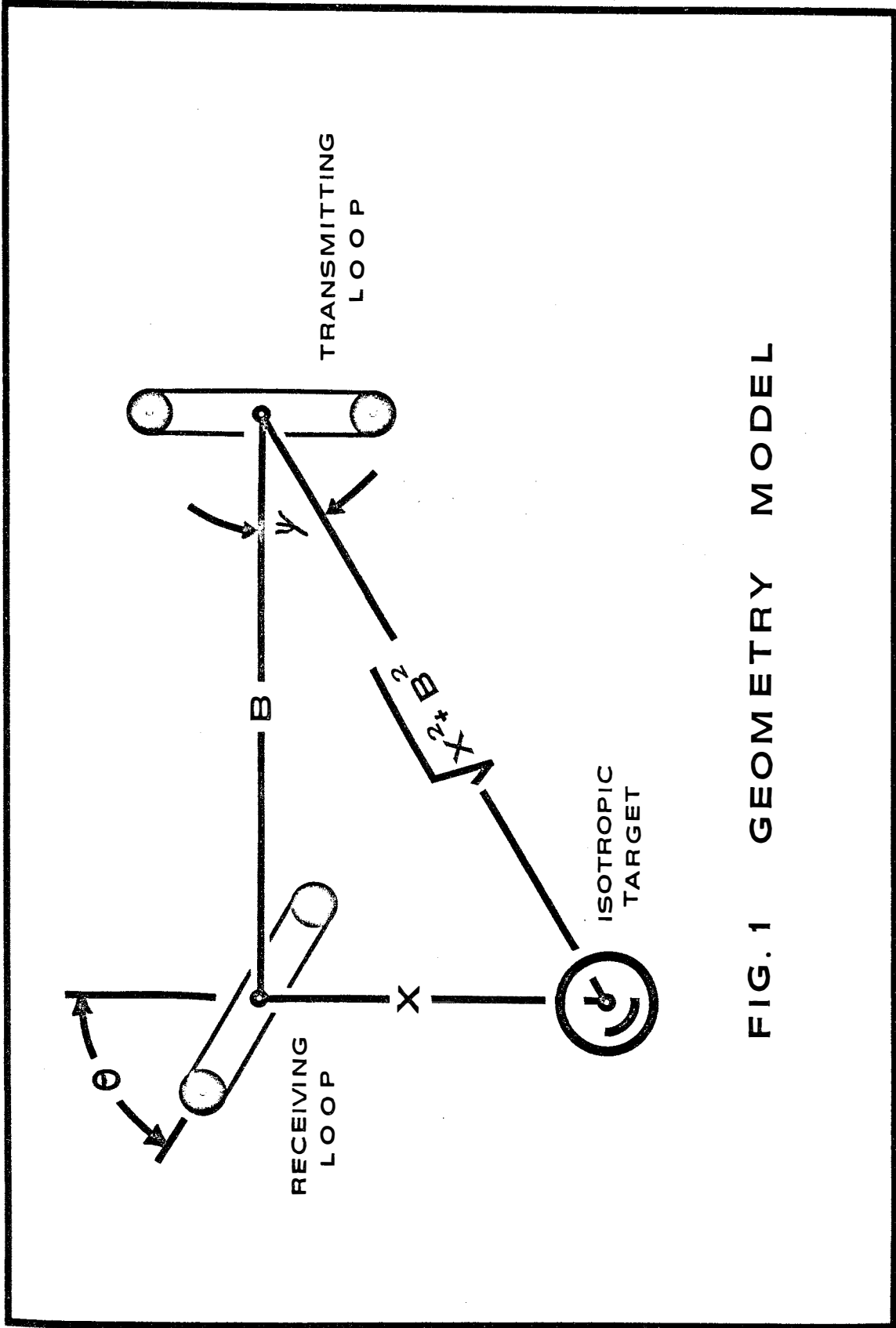


FIG. 1 GEOMETRY MODEL

$$K = \frac{4}{3} \left[\frac{\sqrt{AD}}{r} \right]^3 \quad (1)$$

where

A = diameter of loop, feet

r = radial distance from antenna

taken along an axis of maximum coupling. The coefficient of coupling k_1 between transmitter and target will be attenuated further by $\sin \psi$, where ψ is the target depression angle. Noting that

$$\sin \psi = \frac{x}{\left[B^2 + x^2 \right]^{1/2}}$$

and that

$$r^3 = \left[B^2 + x^2 \right]^{3/2}$$

k_1 will then be given by

$$k_1 = \frac{4}{3} (AD)^{3/2} \frac{x}{\left[B^2 + x^2 \right]^2}$$

For a true 90 degree orientation of the receiving loop when centered above the target, maximum target to loop coupling exists, and the coefficient of coupling k_2 between target and receiver is given by

$$k_2 = \frac{4}{3} (AD)^{3/2} \frac{1}{x}$$

The transmitter to receiver coupling via the target will be given by the product of k_1k_2 as given by

$$k_1k_2 = \frac{16}{9} (AD)^3 \frac{1}{x^2 [b^2 + x^2]^2} \quad (2)$$

The received voltage will be directly proportional to Equation (2) since k_1k_2 and the loop inductances will define the mutual inductance from transmitter to receiver via target.

For large x the receiver voltage for a given target falls off as $1/x^6$ just as in the induction balance and beat frequency locators. For distances small compared to B , the rate of signal drop off as a function of depth follows a much less severe $1/x^2$ law, allowing the detector to retain good sensitivity to depths comparable to B . The price paid for this increase in detectability is a loss in resolution to small objects. As with all inductively coupled locators, the receiver signal increases as the cube of the target diameter.

The optimum value of B is a function of the maximum desired depth of effective penetration contrasted against the minimum allowable resolution to small objects. A plot of the receiver voltage normalized to a given target of one-foot depth for various B and x appears as Figure 2, plotted both in terms of decibels of received signal, and as ratios of target diameters required to produce an equal strength signal.

The loss of resolution as a function of B appears as Figure 3, plotted as the ratio of diameters of targets required for equal detectability.

The presence of a conductive target will not only increase the mutual coupling between the loops but will simultaneously shift the phase of the received signal because of a resistive loss component introduced as the target lowers the "Q" of the coupling system.⁴ Synchronous detection can thus be employed to detect only the real component of the received signal, greatly adding to the detectability. If a

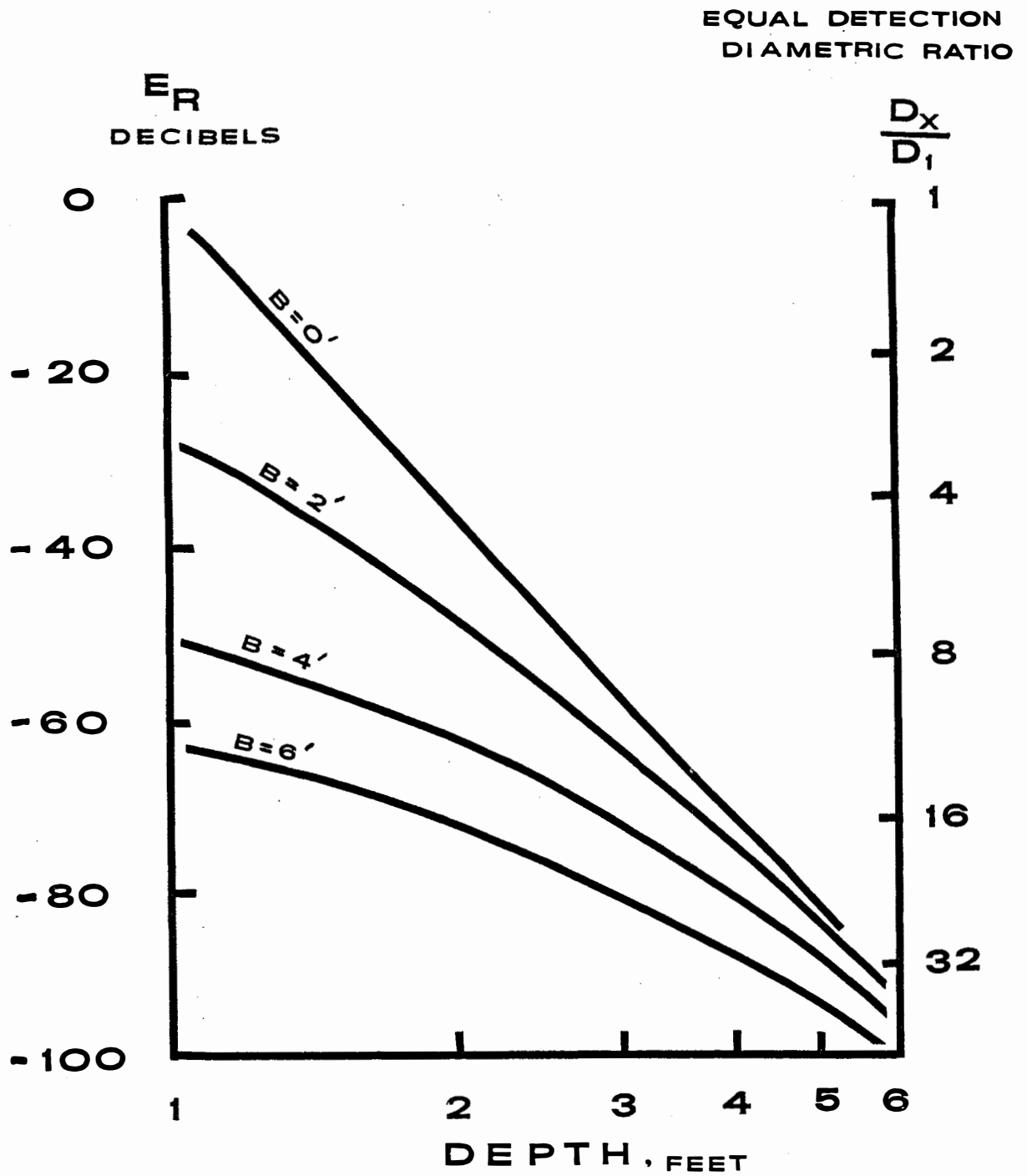


FIG. 2 DETECTION VS DEPTH

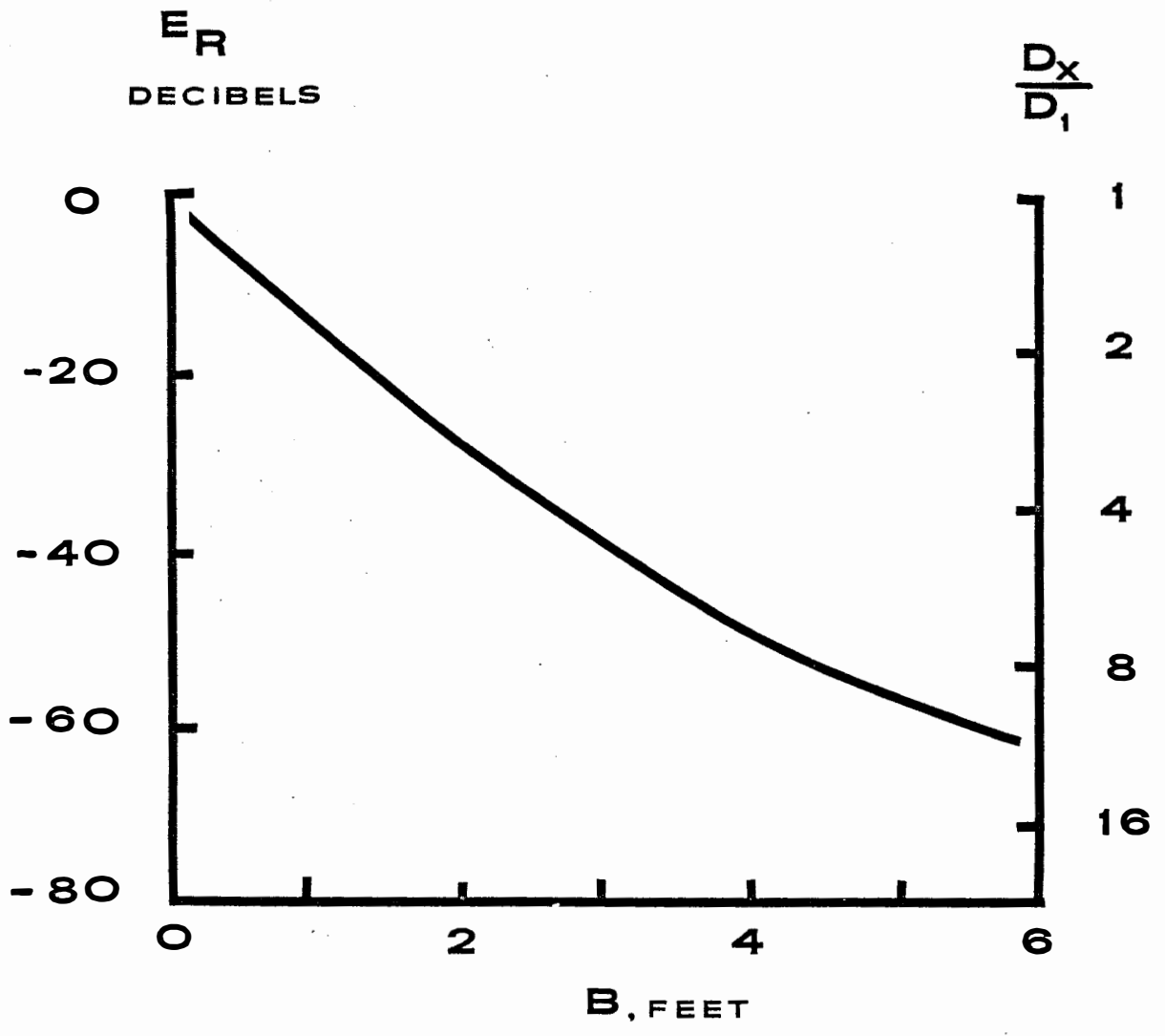


FIG. 3 B vs RESOLUTION

synchronous system is not used, the limiting detectability will be that of a target whose mutual inductance equals the mutual inductance caused by straight-through coupling, ground return, and pattern distortion caused by the circuitry.

The mutual inductance caused by angular misalignment of the loops is given by $M \cos \theta$, where M is the mutual inductance between two parallel loops of diameter A and spacing B sharing a common axis. M is obtained by making use of the extensive tabulations available. Grover's⁵ table 17 is directly applicable and is plotted as Figure 4.

The induced receiver voltage will be given by

$$E_r = M\omega I_{rms} \quad (3)$$

where I_{rms} is the transmitting loop current assuming single turn transmitting and receiving loops.

Since two mutual inductances are involved in target detection, the induced receiver voltage due to a target increase as the square of the frequency used. The highest possible operating frequency, consistent with terrestrial absorption, must be used to obtain maximum target sensitivity.

The model locator was designed with pipe location as a primary goal, requiring effective penetration to four feet of depth and better. A value of $B = 4'$ and $A = 1'$ was selected.

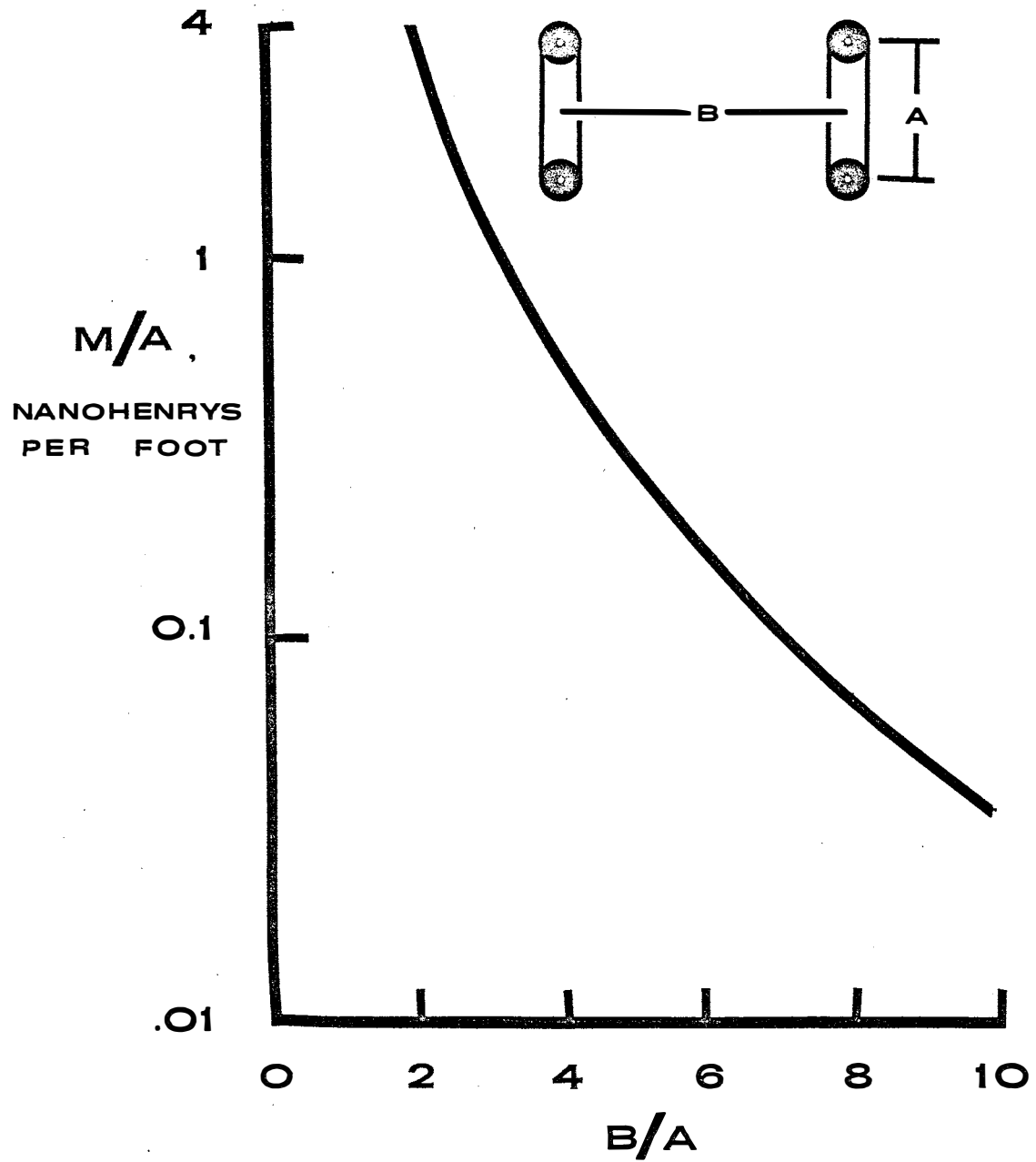


FIG.4 INDUCTIVE LOOP COUPLING

CHOICE OF FREQUENCY

The effects of terrestrial absorption and the locator detectability requirements interact to determine a suitable operating frequency.

Terrestrial absorption will reduce E_r further as a function of depth by a factor of αy where α is the attenuation per foot in decibels and y is the round trip terrestrial distance. Total terrestrial attenuation is then given by

$$\text{Attenuation} = \alpha \left[x^2 + \left[b^2 + x^2 \right]^{1/2} \right] \quad \text{Decibels} \quad (4)$$

A plot of the received E_r that takes into account various values of α is plotted as Figure 5 for $B = 4$ feet.

The terrestrial absorption will vary with frequency as well as the resistivity and dielectric constant of the earth at the point of penetration. Heiland⁶ has shown that the low-frequency penetration equations are valid except for very high frequencies and soil resistivities, and that the results are always conservative for any frequency and conductivity.

One form of the low-frequency equation is

$$d = 60 \left[\frac{\rho}{f} \right]^{1/2}$$

where

$d = 1/\epsilon$ penetration in meters

$\rho =$ resistivity in ohm-centimeters

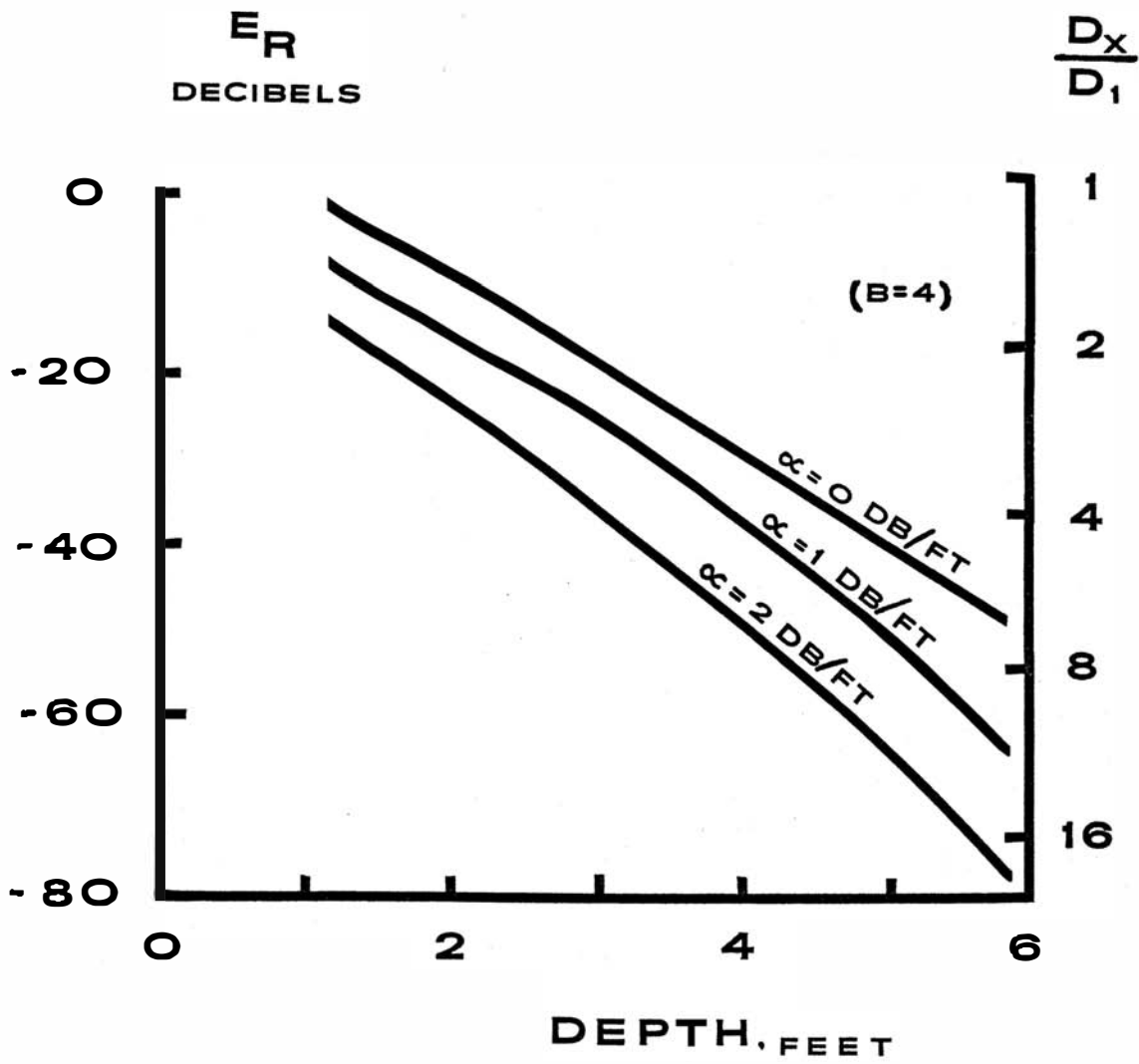


FIG. 5 E_R vs ATTENUATION

as taken from Heiland's Figure 10-24. At $1/\epsilon$ attenuation, the loss is 8.7 decibels. By changing dimensions, the inverse relation

$$\alpha = 0.045 \left[\frac{f}{\rho} \right]^{1/2} \quad (5)$$

is obtained with α expressed in decibels/foot.

Values of resistivity for different media are taken from Heiland's text and plotted as a function of frequency in Figure 6. The curves indicate an excessive amount of attenuation for most media at frequencies above 500 kHz. 455 kHz is within a tolerable attenuation region and both favors the receiver sensitivity requirements and makes optimum use of available components. This is the operating frequency chosen for the evaluation model.

Neglecting the dielectric constant in the above analysis will have two opposing consequences. At the frequencies used, high values of k serve to decrease the terrestrial absorption, acting much as a bypass capacitor to allow the high frequency energy to more freely travel through a lossy media. At the same time, large values of k introduce a substantial mismatch between the loops in air and the earth-air interface, and can cause a ground reflection that could constitute a significant portion of the total transmitted energy. Values of k encountered can be extreme, owing to water having a dielectric constant of 84 and most soils having a moderate to substantial moisture content.

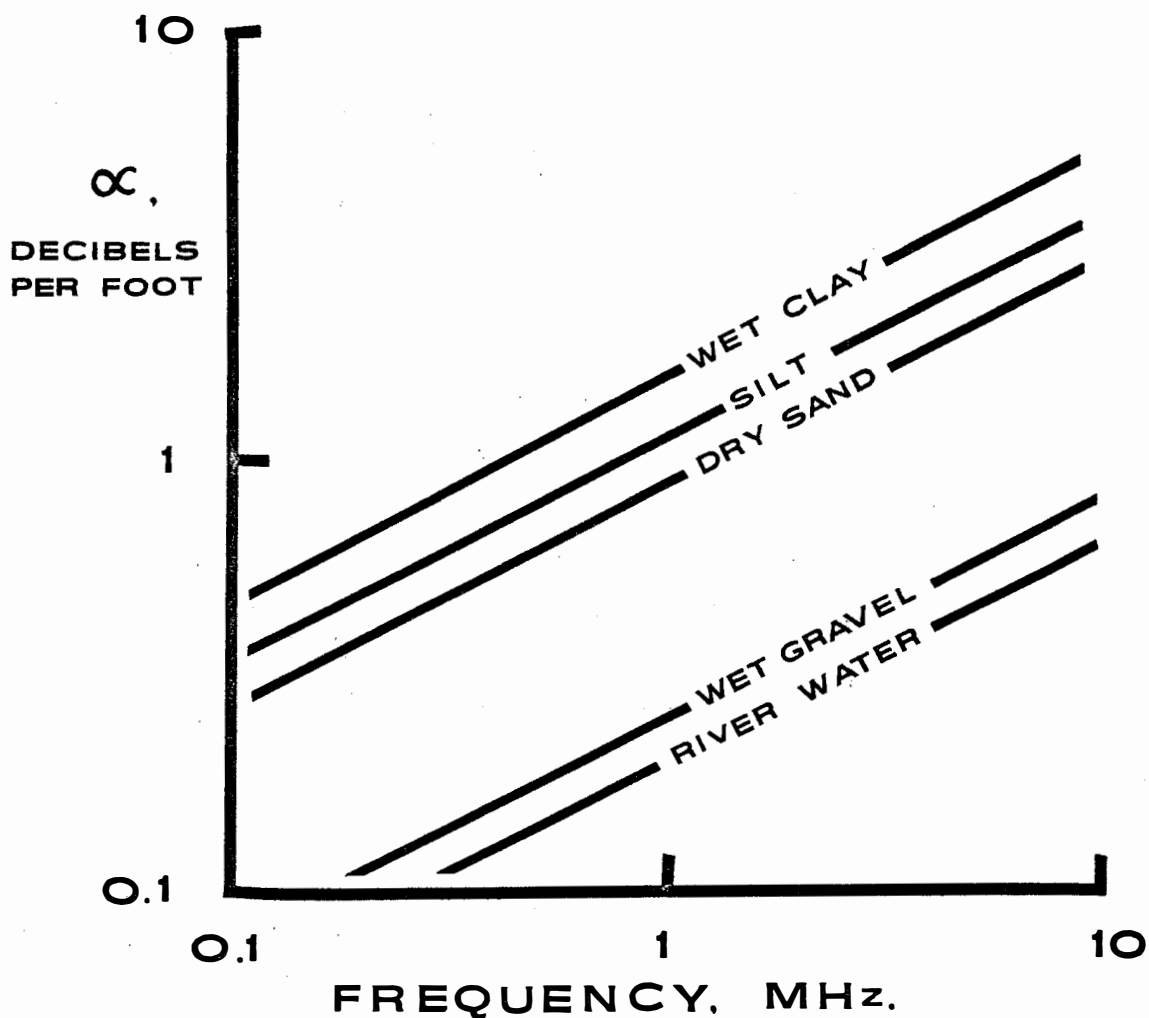


FIG. 6 TERRESTRIAL ATTENUATION

RECEIVER SENSITIVITY AND BANDWIDTH

The receiver sensitivity may be interpreted in terms of that signal induced in the receiving antenna for a one-degree angular misalignment of the receiving loop from true null.

Resonant loops are used for both receiver and transmitter to allow Q multiplication of transmitter current and receiver voltage. To place all metal used in the locator at neutral potential, balanced loops are employed.

Several techniques were tried for the loop assemblies, the most practical of which was a 10 inch by 12 inch oval loop of four conductor number 18 AWG communication cable, rewired by sequential connection to produce a four turn, center tapped configuration. The unloaded loops gave Q's of 65, which dropped to 30 when driving a 2000 ohm load. The inductance is 18 microhenries which requires 6800 picofarads of capacity to resonate at 455 kHz. To allow for final tuning, a 700-picofarad trimmer is placed in parallel with 6500 picofarads of fixed capacity. Identical geometry is employed for both loops.

The received signal due to straight-through coupling is given by

$$E_r = -jMN_t N_r Q_t Q_r \omega \frac{E_t}{r_p} \sin \theta \quad (6)$$

where

N_r = number of receiving loop turns

N_t = number of transmitting loop turns

Q_r = loaded receiver loop Q

Q_t = Loaded transmitter loop Q

r_p = equivalent parallel resistance of transmitting loop and oscillator

E_t = RMS voltage across transmitting loop.

For a one-volt RMS E_t across 1000 ohms and values of $Q_t = 15$ and $Q_r = 30$, a receiver sensitivity requirement of 73.5 microvolts results. A full output from 100 microvolts of input may then be defined as a receiver design objective.

The receiver bandwidth is not overly critical, and is chosen to be narrow, while still allowing fixed tuned RF stages using ordinary ± 10 percent capacitors. A 70 kHz, 15 percent bandwidth may be selected using this criterion. The over-all selectivity and noise rejection would then be defined by the receiving loop and the first RF stage impedance characteristics. Using $Q_r = 30$ results in a 3 decibel system bandwidth of 18.2 kHz.

SIGNAL PROCESSING TECHNIQUES

Two of the methods that may be applied to enhance the detection capability of an electronic locator are synchronous demodulation and non-linear signal processing. Because of the 90 degree phase difference between the real part of a conductive target return and the normal inductive coupling, a synchronous system may be used to substantially reduce the straight-through coupling as well as much of the return from the earth-air interface. In such a system, the receiver output is demodulated synchronously in phase with the transmitter reference, rejecting the unwanted quadrature signals and returning only the inphase return from a buried conductor.

Certain limitations have prevented the use of synchronous techniques to date on the receiver transmitter type of locator. These limitations take the form of pattern distortion, stability restrictions, and a reduction in utility due to the receiver and transmitter being permanently connected together. The pattern distortion problem is the most severe. The wire interconnections between transmitter and receiver must of necessity intercept some transmitter energy and thus distort the field pattern. By keeping the interconnections directly along the null axis of the loop as much as possible, this form of distortion may be minimized. A related problem is caused by the connected wires themselves radiating. This may be eliminated by using balanced receiver, transmitter, and demodulator configurations, and by thoroughly shielding the interconnections.

For a minimum of 20 decibels of straight-through rejection, the total system phase shift must be set and held to ± 6 electrical degrees. For 40 decibels of rejection, the total drift must be held to less than ± 0.6 degrees and the system dynamic range and demodulator quadrature

rejection must well exceed this figure. The ultimate limiting factor in attainable improvement is dictated by the real term neglected in Equation (1). For a 455 KHz frequency and a 50-inch spacing, the ultimate attainable improvement using synchronous techniques is approximately 40 decibels. Thus, a reasonable improvement may be expected using a relatively simple synchronous system, but an extensive increase in detectability may only be obtained with an elaborate system using wideband circuitry, logarithmic amplifiers, and carefully balanced loops and demodulators.

Two unique advantages of the receiver-transmitter locator are the ability to track a buried pipe and the ability to triangulate for a depth indication. Both of these potential advantages require that the transmitter and receiver be totally separated without any disabling effects. It would then appear that a selectable dual demodulation system is of advantage, one synchronous and one asynchronous.

A large degree of clutter rejection independent of phase relationships may be obtained by nonlinear processing of the detected signal, and elaborate systems of this type are employed in certain military UHF mine locators.⁸

Figure 7 shows a relatively simple means of nonlinear processing. If a very high β transistor is driven from a voltage source, a nonlinear transconductance characteristic is produced. In operation, the detected and filtered receiver output E_r is summed with the base bias voltage and the collector current is then taken as the output.

If the stage is biased to point A (Figure 7), linear amplification is obtained with all signals being equally amplified. This operating point also corresponds to a maximum sensitivity condition, brought about by a maximum stage gain and a prebiasing effect of the base current upon the detection circuitry.

Operation at point B will produce a squelch mode of operation in which no output will be obtained unless the return from a large target is received. This mode is of primary utility when tracing a single known target.

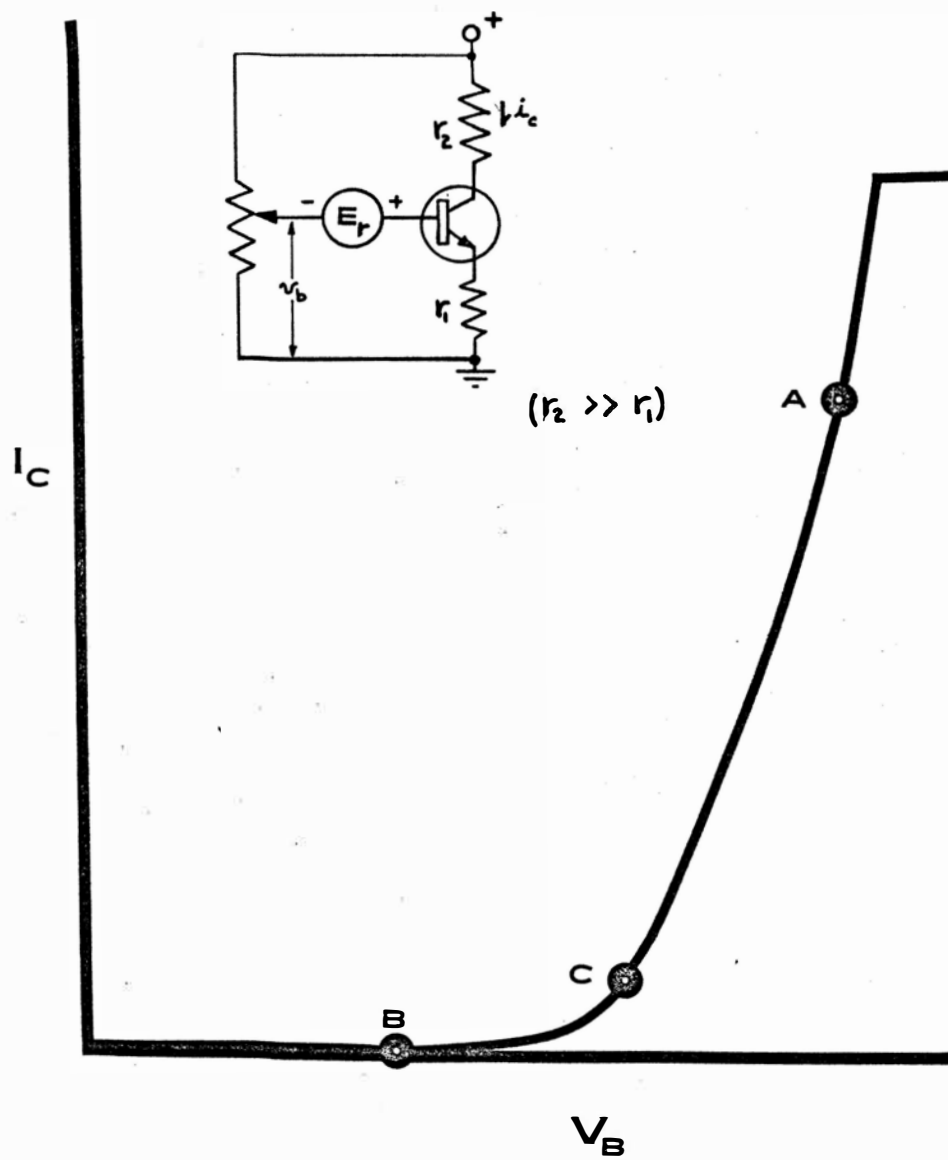


FIG. 7 EXPANDER CIRCUITRY

By biasing on the knee of the curve (point C) low level signals will not be amplified as much as higher level ones, thereby providing expansion to target signals while suppressing normal background clutter.

In the demonstration model, the signal expander stage forms a permanent part of the circuitry, while the remainder of the circuit is designed to allow either linear or synchronous detection. The model was built and initially evaluated on a nonsynchronous basis.

SYSTEM BLOCK DIAGRAM

The block diagram appears as Figure 8. The transmitter consists of a balanced CW oscillator driving a vertical transmitting loop, coupled to a mechanical null adjuster to provide precise control over the null axis.

An identical horizontal fixed loop forms the receiver front end, followed by three stages of tuned RF amplification, required to bring the 100 μ volt received signals up to a level suitable for linear diode detection or synchronous demodulation. For synchronous operation, a balanced reference is derived directly from the oscillator.

Detection is followed by the expander circuit of Figure 7, which in turn drives both a 0-1 DC milliammeter and an integrated sonic alarm module,⁹ providing both visual and aural output indication.

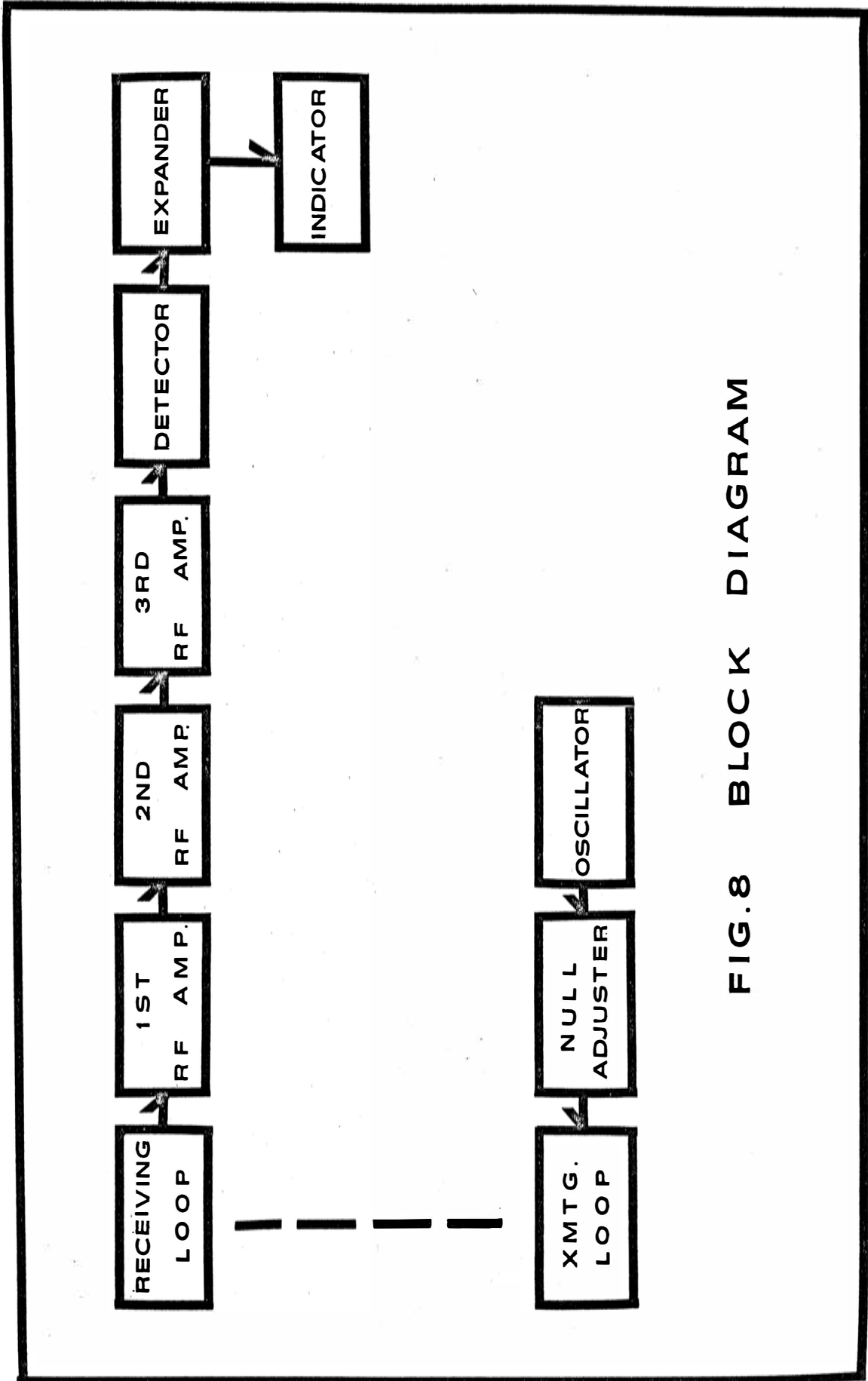


FIG.8 BLOCK DIAGRAM

USE OF INTEGRATED CIRCUITRY

Integrated circuitry is employed for all stages except that of the signal expander, which makes use of a single, high gain silicon transistor. Dual two-input logic gates are modified to form linear differential amplifiers that serve as oscillator and the first three RF stages, while a commercially available "integrated" sonic module is employed as a replacement for the audio circuitry.

The integrated circuit selected was the Fairchild μ L914, a dual two-input logic gate readily converted into a linear amplifier by using only one input on each side and driving the emitters from a negative current source.¹⁰ The unused internal transistors are bypassed by connecting their bases to the common emitter point.

The basic differential amplifier configuration is shown in Figure 9.¹¹ Normal use of this circuit requires a true current source at the emitters to ensure significant common mode rejection as well as a matched pair of transistors. The fact that integrated circuitry is used guarantees that both transistors will be at the same temperature and that both will have nearly identical characteristics.

Referencing both input bases to ground via a low DC impedance eliminates the common mode signal problem, allowing a simple resistor and negative 3-volt supply to replace the current source. Transformer coupling of outputs forces the average collector voltage to be V_{CC} , independent of any initial current unbalance, resulting in a stable yet extremely simple circuit.

An input e_1 drives an emitter follower which in turn drives a grounded base stage to arrive at the right output, while the input e_2 drives the same circuit as a common emitter stage. Together the two produce the composite right output $K(e_1 - e_2)$. The opposite, or difference signal appears at the left and is given by $K(e_2 - e_1)$.

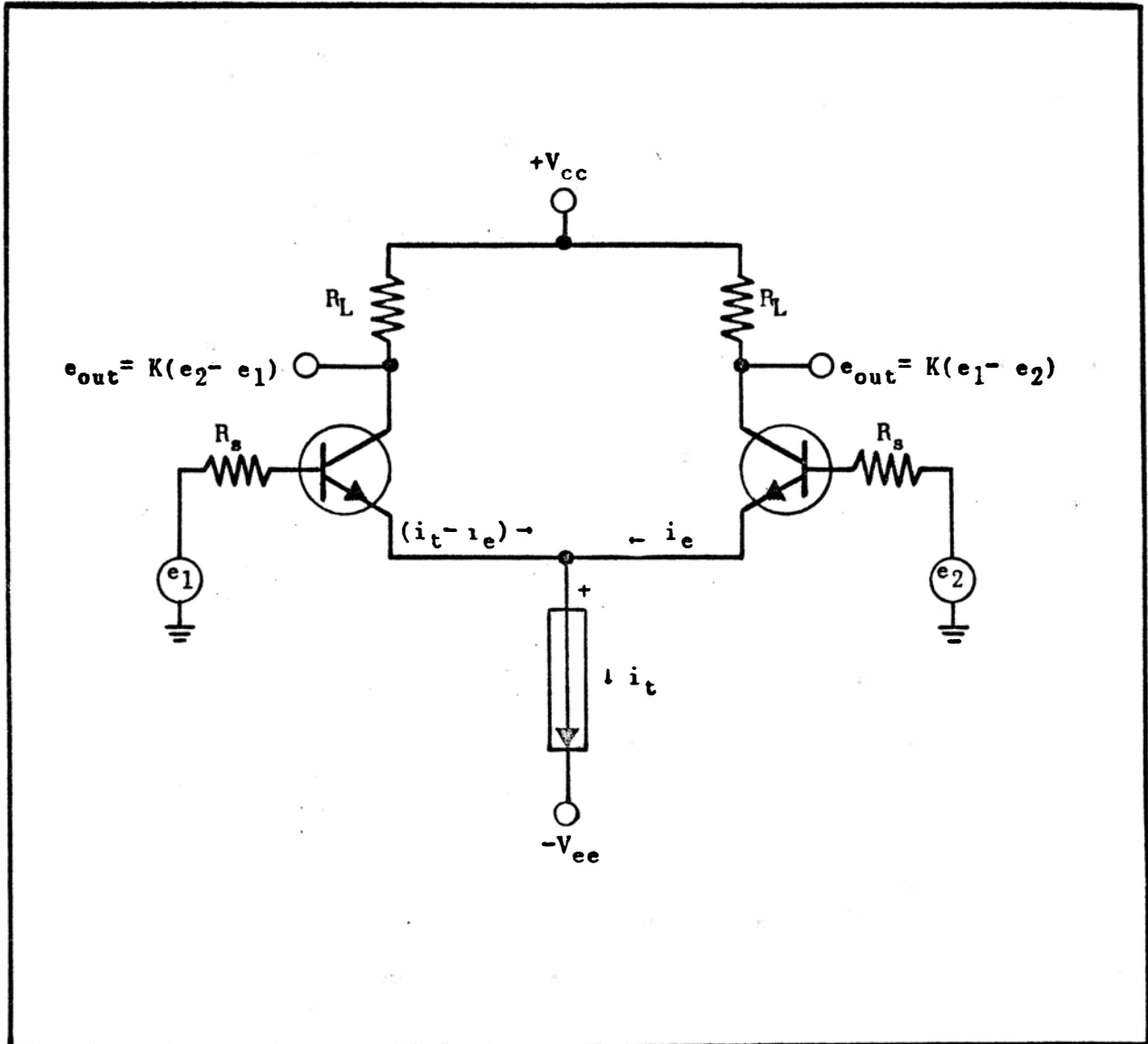


FIGURE 9 - BASIC DIFFERENTIAL AMPLIFIER CONFIGURATION

The voltage gain is a function of the emitter current and the collector load impedance. The input impedance of a common base stage is approximately

$$r_{be} = \frac{26}{i_e}$$

where

$$\begin{aligned} r_{be} &= \text{input impedance in ohms} \\ i_e &= \text{emitter current in milliamperes.} \end{aligned}$$

The voltage gain of a common base stage is in turn given by R_L/r_{be} where R_L is the collector load resistance. The total gain of the differential stage is then given by

$$\frac{E_{out}}{E_1} = \frac{R_L i_e}{26} \tag{7}$$

with i_e being one-half the total emitter bias current i_t under no-signal conditions. The expected gain performance for the $\mu L914$ is plotted in Figure 10 as a function of emitter current and load resistance. Up to 34 decibels of stage gain may be obtained using a two milliamperere emitter bias current source. The two internal resistors of 640 ohms each fix the maximum possible value of R_L at 640 or 1280 ohms, depending upon the choice of collector connections.

The gain is easily controlled by varying the emitter current. For very low values of i_e , the R_L/r_{be} ratio is less than unity and a negative stage gain results.

The input impedance is given by

$$R_{in} = \beta r_{be} \tag{8}$$

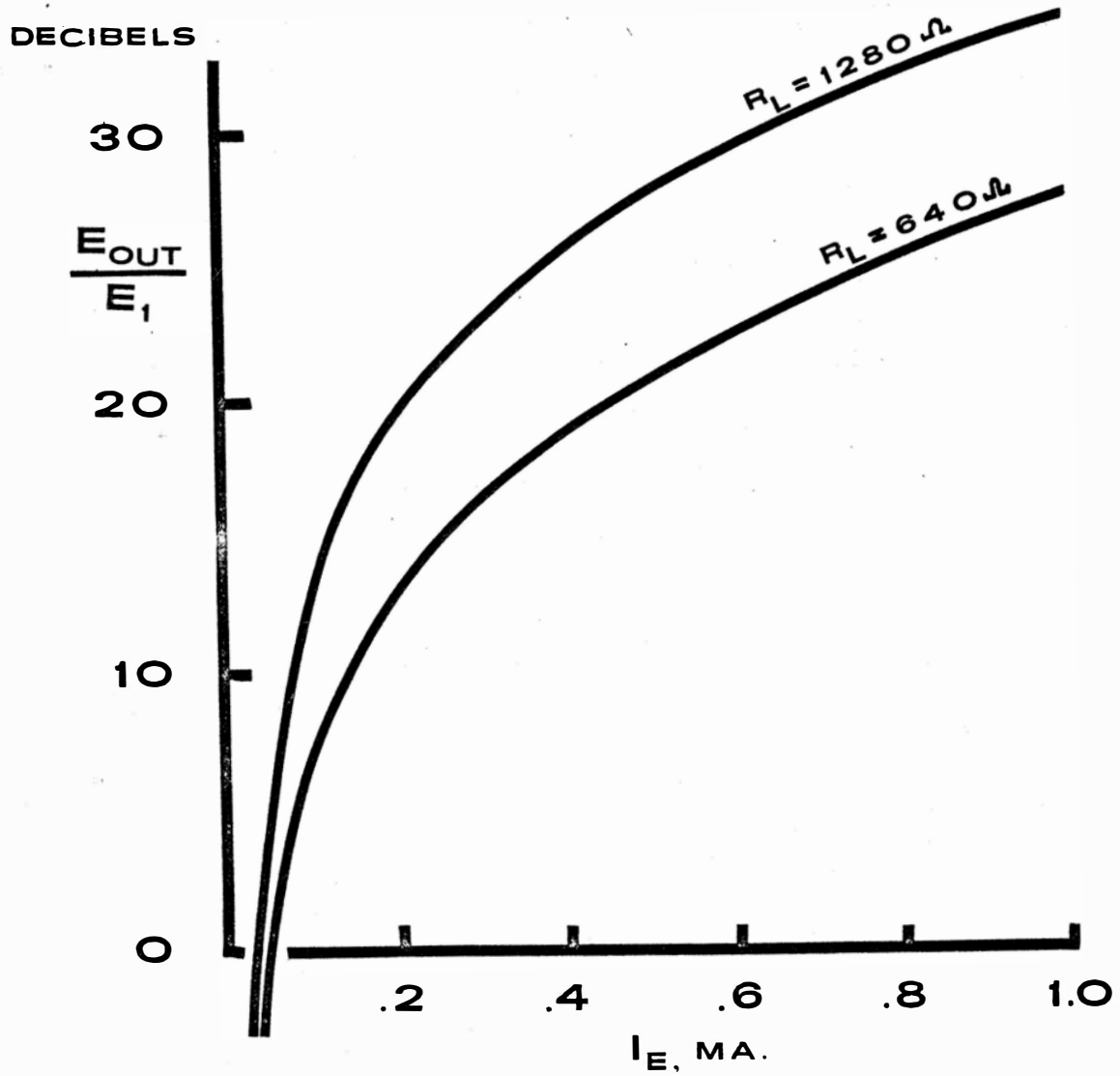


FIG. 10 SINGLE STAGE GAIN

where β is the current gain or h_{fe} of the equivalent transistors. R_{in} is plotted for various β in Figure 11. Experimental RX bridge measurements on several $\mu L914$ integrated circuits were made over the range of 500 kHz to 10 MHz. The resultant room temperature values of β were in the range of 50 to 80, producing input impedances above 2000 ohms for all but the highest values of i_e . Since the input impedance is a function of the emitter current, the interstage design must provide a relatively low source impedance and consequent power mismatch, lest the changing input impedance affect the bandwidth and stability of the system.

The differential amplifier configuration is also an effective limiter and operation in the limiting mode would be highly detrimental to the detection problem. Limiting takes place when the total bias current i_t is routed to one output. The total possible peak-to-peak output swing is given by $i_t R_L$ and the peak output is given by

$$E_{out\ peak} = \frac{1}{2} i_t R_L \quad (9)$$

which is plotted in Figure 12 as a function of load resistance and bias current. If a large nonlimited output swing is to be obtained, the third RF amplifier must be operated at a fixed high gain, for any attempt of gain control on this stage will be met with amplitude limiting problems.

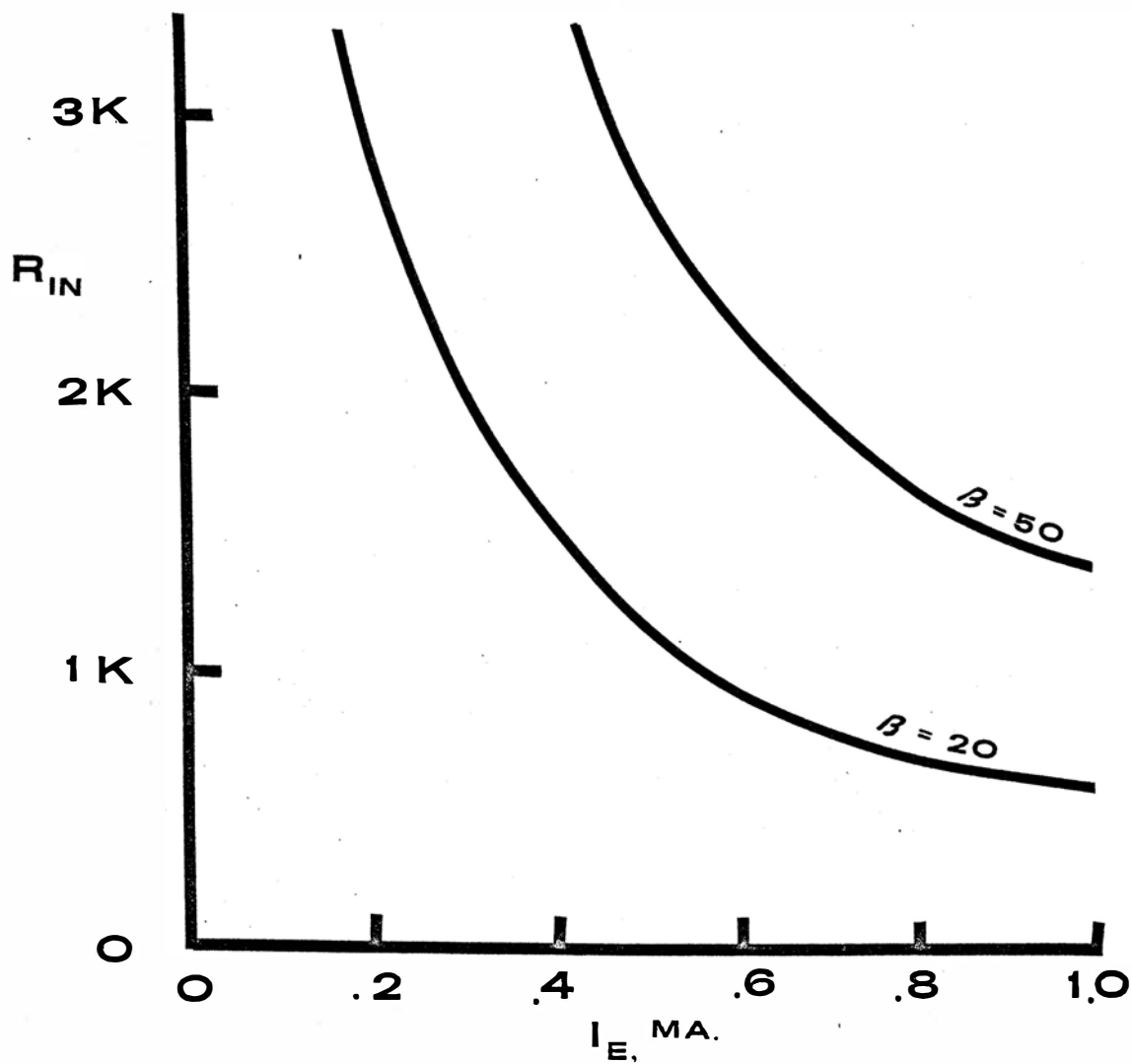


FIG. 11 INPUT IMPEDANCE

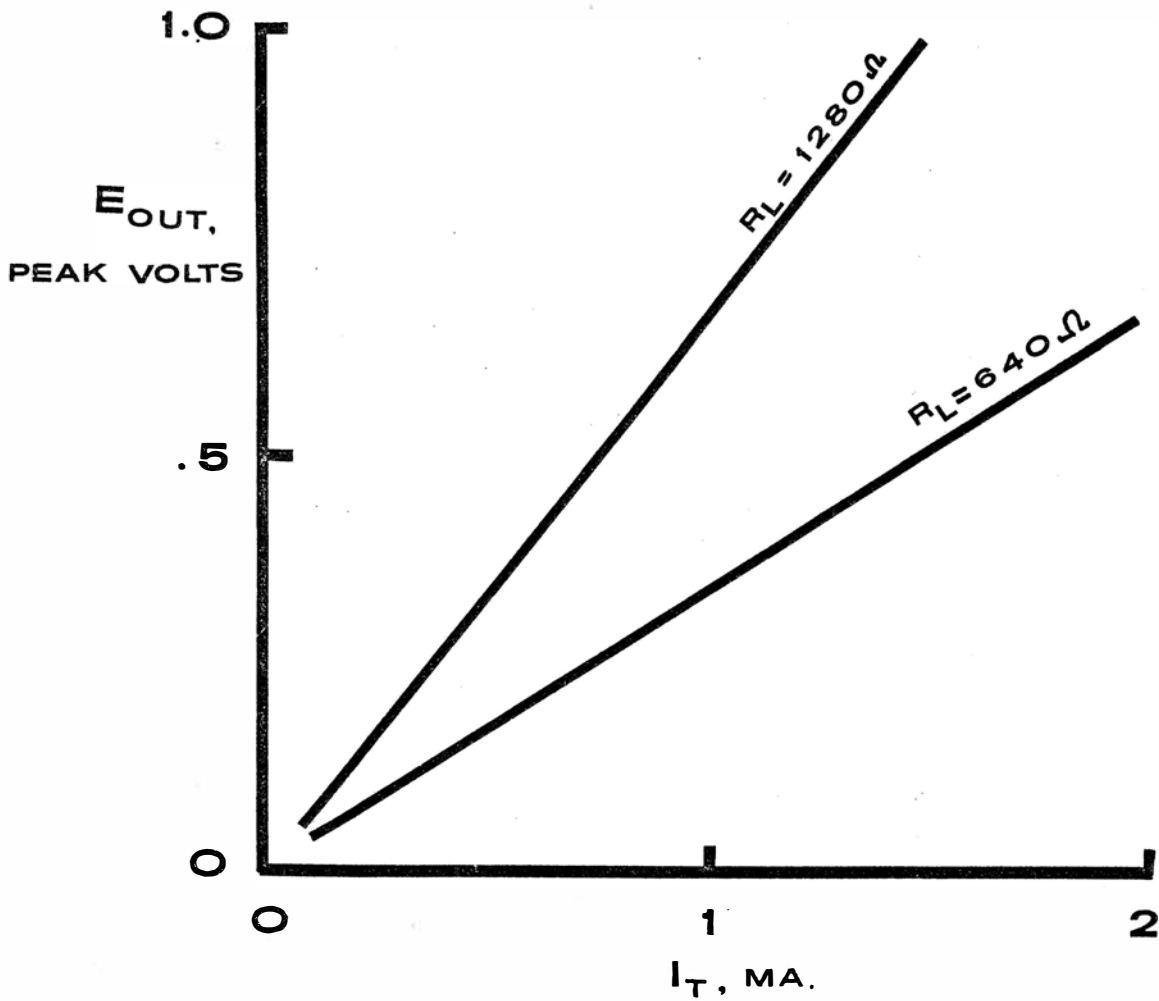


FIG 12 MAXIMUM OUTPUT

COMPLETE SCHEMATIC

The complete schematic for a nonsynchronous integrated locator is given in Figure 13. The transmitter consists of a balanced CW oscillator, formed by using the resonant center-tapped transmitting loop as both collector loads for a single μ L914. A 455 kHz ceramic resonator (transfilter) is cross-coupled from one collector to the other base to provide a feedback path. The resonator selected has an input impedance of 2000 ohms, an output impedance of 300 ohms, and a power insertion loss of 2 decibels. Although lower in cost, the stability of this circuit is not much worse than that of a crystal oscillator.

A three position OFF-LOW-HIGH switch chooses one of the two emitter resistors providing transmitting loop voltages of 0.8 and 3 volts peak-to-peak. The LOW position is normally employed for outline purposes after a target has been located.

The receiver design philosophy is similar to that of Robertson.¹² A μ L914 forms the first RF amplifier, being driven in a balanced manner by the center-tapped receiving loop assembly. A single-ended output is produced. Interstage coupling is by means of 1:1 bifilar wound torodial transformers whose primaries are resonated at 455 kHz. The interstage Q is set to 8, allowing fixed tuning.

Indiana General Type Q1 material is used for the cores, combining a low cost with a permeability of 125, a high Q at the operating frequency, and a temperature coefficient of 0.1 percent per degree Celsius.

Since the internal collector resistors are smaller than the input impedance of the following stage, the system bandwidth is largely independent of the per-stage gain.

The second RF amplifier consists of a μ L914 operated with single-ended input and output. The first two RF stages are gain controlled by means of a variable 3 volt negative emitter supply. A deliberately introduced potentiometer loading error serves to linearize gain as a function of knob position.

The third RF stage differs from the second only in the use of a fixed gain and a lower value collector resistor. The lower output impedance is required to provide a suitably low power impedance for the detector stage. A conventional germanium diode detector follows the third RF stage, which in turn drives the expander circuit.

Several measures are taken to insure receiver stability. The power supplies are decoupled by means of nonresonant ferrite bead chokes and quality bypass capacitors. The phase of the received signal is reversed at each transformer secondary to minimize positive feedback. As two final precautions, the entire RF portion of the receiver is placed between two ground planes designed as a waveguide far below cutoff to attenuate any electromagnetic coupling from high to low level stages. The entire receiver is built inside an RF neutral aluminum case to prevent any output signals from direct coupling into the receiving loop assembly.

Six AA penlight cells are required for power. The two in the transmitter deliver 4.5 milliwatts of per-cell power in the HIGH position. The maximum per-cell receiver power requirement is 18 milliwatts with the sonic module in use and 9 without. The receiver cells are tested by biasing the expander stage to saturation and noting the meter deflection, while the transmitter cells are tested by metallic detection or misalignment of the mechanical null adjuster control.

Synchronization may be achieved by the circuit of Figure 14. A balanced transmission line is used to drive a four diode synchronous gate, providing half wave synchronous demodulation of the receiver output. A selector switch would be added to provide a choice of synchronous or nonsynchronous operation.

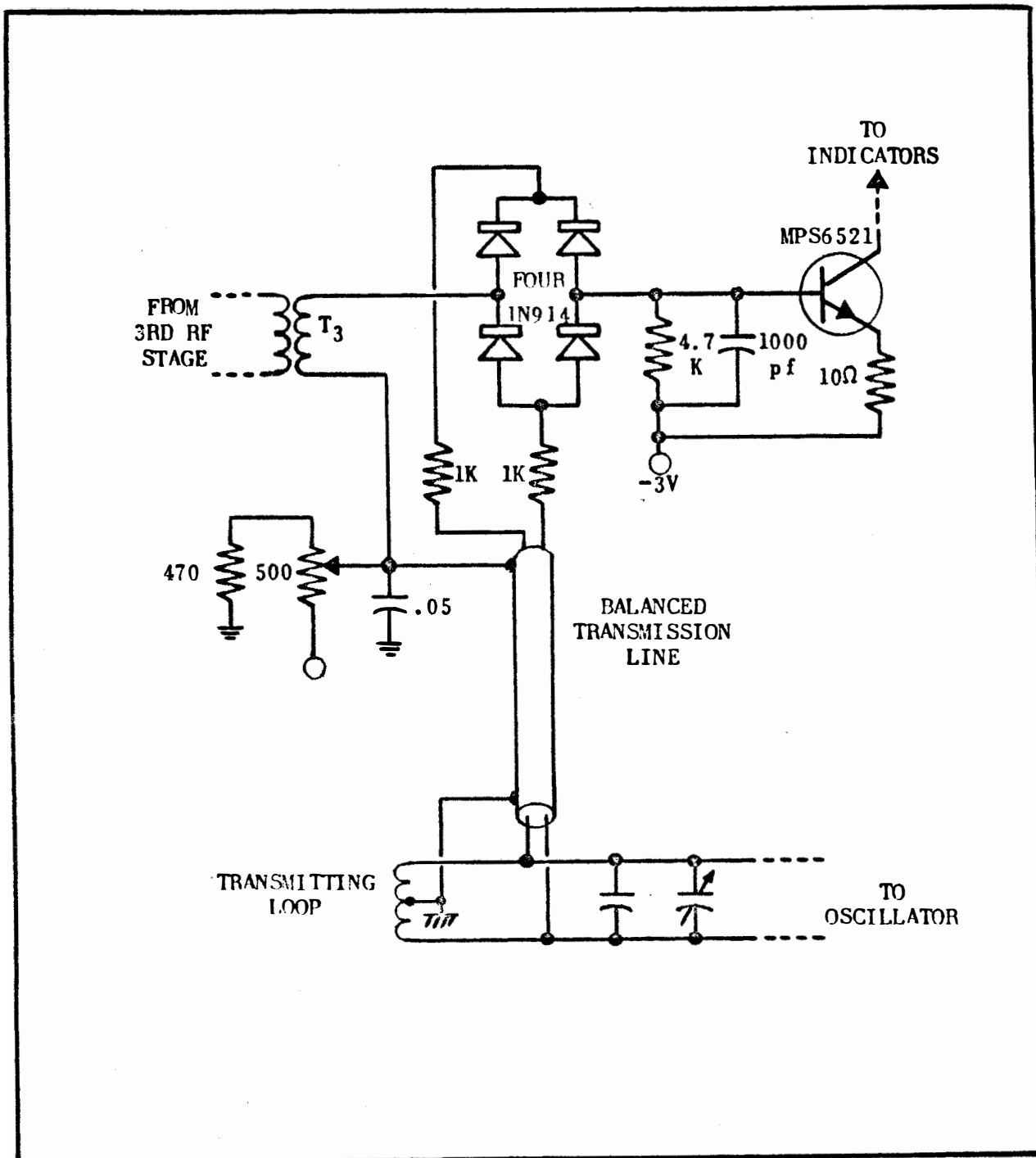


FIGURE 14 - SYNCHRONOUS DEMODULATOR

DEMONSTRATION MODEL

A demonstration model using the schematic of Figure 13 was constructed and appears as Figure 15. The instrument measures 51 inches long and 13 inches wide, and is constructed of a maple main frame and plywood loop support assemblies. Although no attempt was made at minimizing weight, the complete instrument weighs slightly over six pounds, significantly less than that of comparable designs.

The mechanical microbalance adjuster is detailed in Figure 16 and consists of a maple pivot assembly that is adjustable over a ± 15 degree arc by means of a knob adjustment. 0.8 degrees of rotation are obtained for each complete turn of the adjusting knob.

The rear loop assembly is shown in Figure 17 and is removable via four thumb screws. The transmitter of Figure 18 is contained in a 2 1/2 inch square by 1 inch deep aluminum box which mounts directly on the transmitting loop assembly.

The receiving section is outlined in Figures 19, 20, and 21. The front loop assembly is permanently attached to the main frame, as is the 3 inch by 4 inch by 5 inch aluminum case that houses all receiver electronics. The case itself holds the printed circuit RF section and the ground plane assembly, as well as holders for the four penlight cells. A removable cover supports both the indicators and the receiver controls.

To obtain a synchronous detector, additional connectors and a balanced transmission line are added between transmitter and receiver. A modified printed circuit is then used that provides for switch selection of either detection mode.

-36-
Figure 15
Model Locator



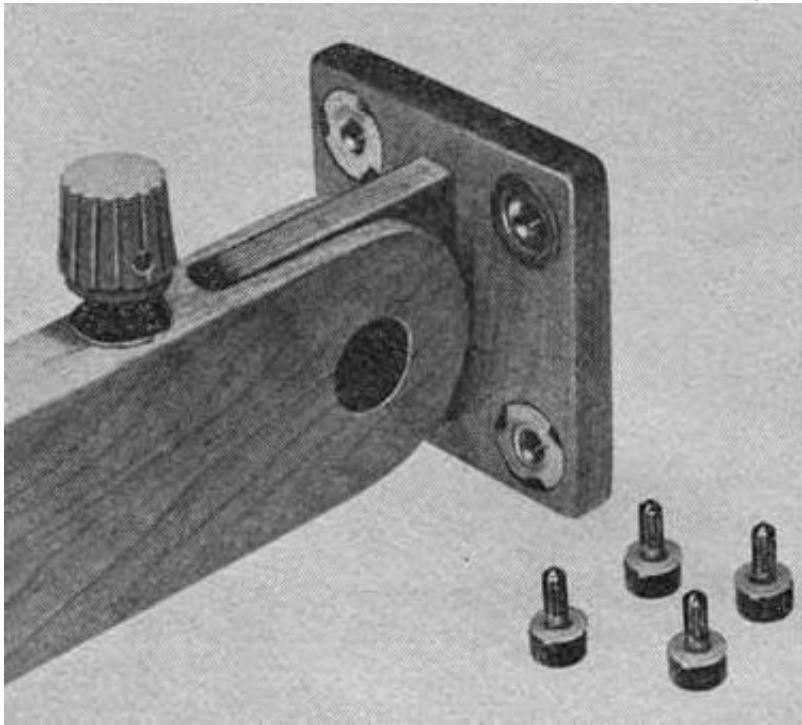


Figure 16 - Microbalance Details

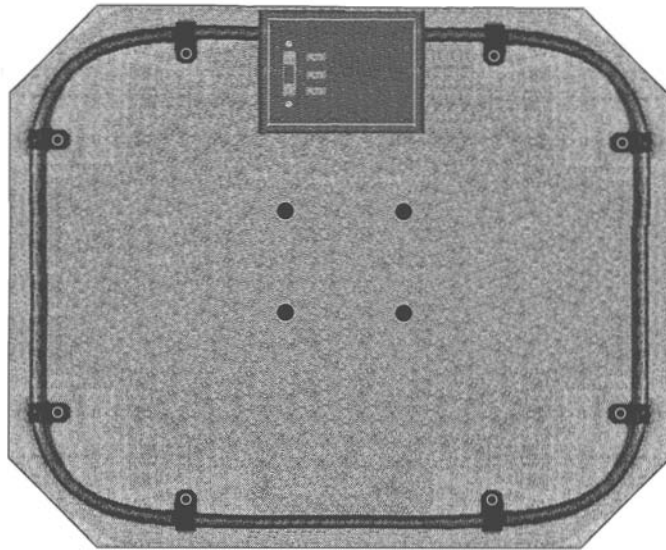


Figure 17 - Rear Loop Assembly

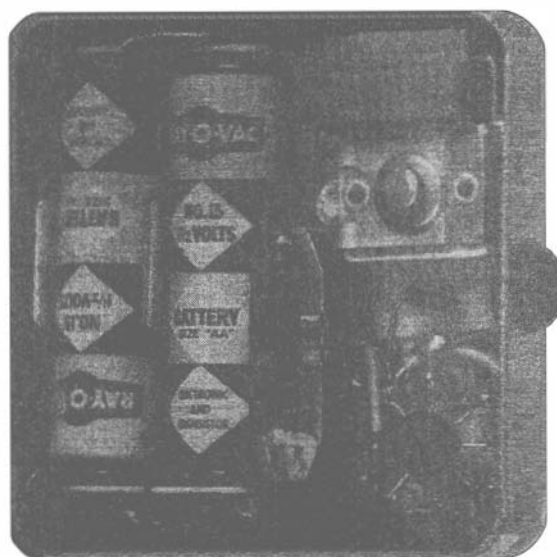


Figure 18 - Transmitter

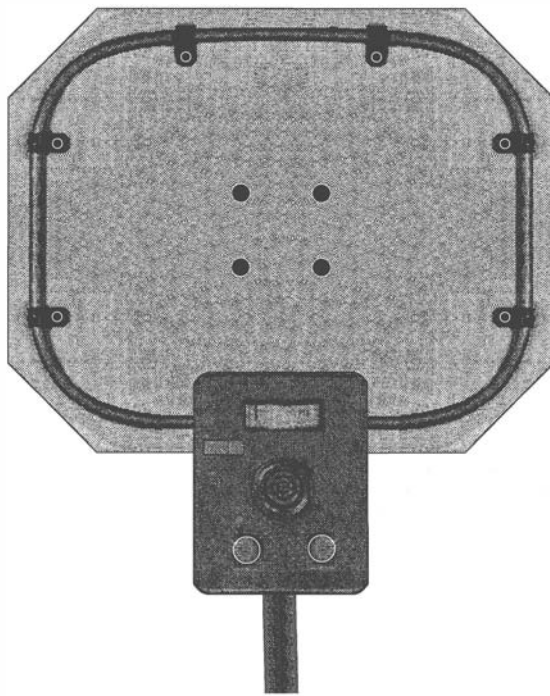


Figure 19 - Receiving Loop Assembly

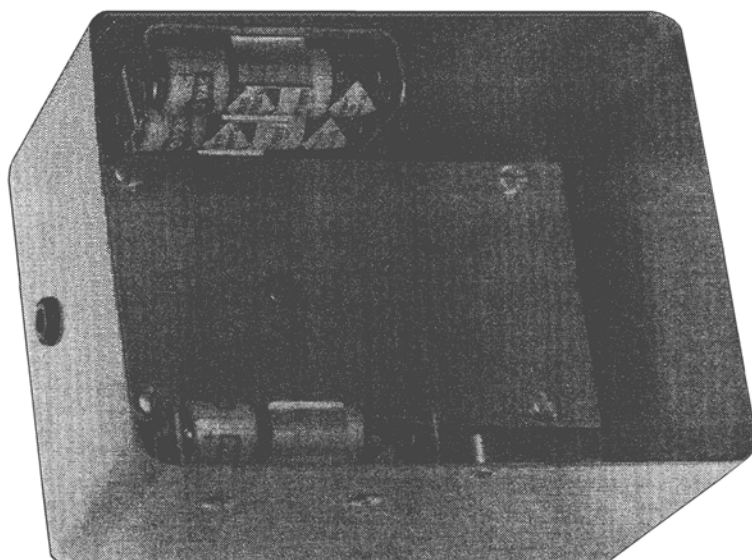


Figure 20 - Receiver Case

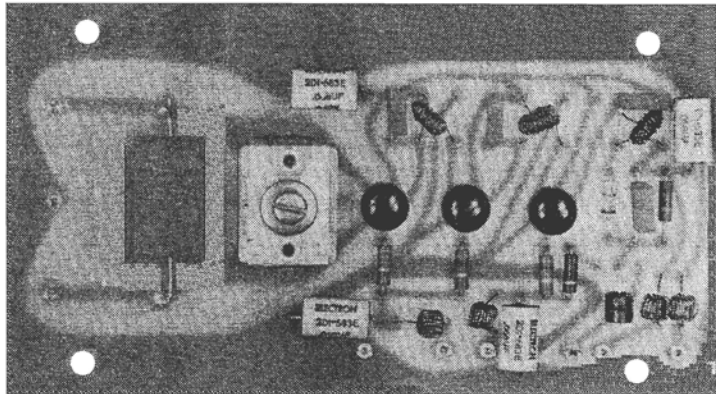


Figure 21 - Receiver RF Printed Circuit Board

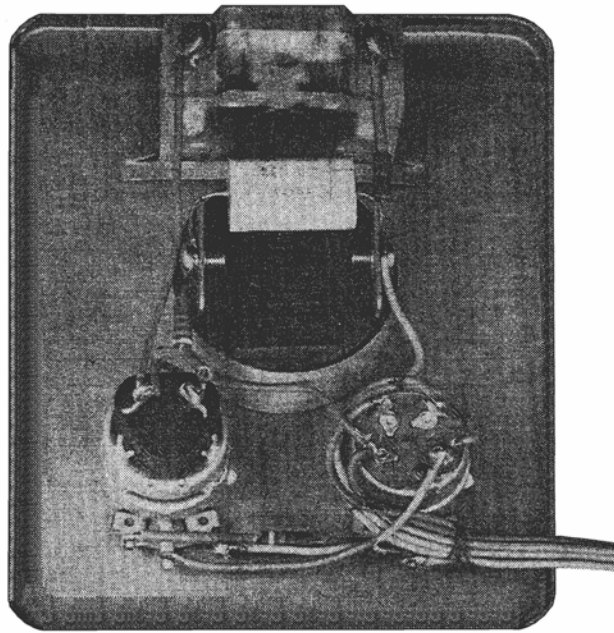


Figure 22 - Receiver Front Panel, Rear View

EXPERIMENTAL RESULTS

Both receiver and transmitter were separately tested and evaluated. Receiver gain is above 90 decibels maximum over a 35 kHz bandwidth centered at 455 kHz. A sharp null is obtained at the 90 degree position of the transmitting loop assembly, indicating a minimum of field distortion has in reality been obtained. Receiver sensitivity is adequate enough to override the best null at maximum gain settings. The receiver is unconditionally stable.

An older military SCR625A induction balance mine locator was used as a standard of comparison.¹³ The integrated locator was found clearly superior on every test performed, with the sole exception of resolution to very small objects. There is a 7:1 weight difference and a 10:1 difference in battery costs between the two units, not considering the substantially longer battery life in the integrated locator.

Eight square feet of metal in air produced a strong response in the integrated locator at a distance of 5 feet; the SCR625 produced very little indication at distances greater than 10 inches. A 48 inch long pipe 1 inch in diameter produced equal detectability on the surface, but when buried to a one-foot depth in sand, the SCR625 all but lost its output signal, while a strong return was still registered on the integrated locator.

Several water lines were easily traced with the instrument, as were city water mains buried over four feet deep. The minimum sized object to produce a detectable return at one foot is a three-inch sphere. The expander circuitry was of definite value in target identification.

Extensive resolution or penetration tests were not yet carried out as initial testing was made on a nonsynchronous basis that is not indicative of the ultimate performance of such an instrument.

FURTHER WORK

Several design areas merit further investigation. The model locator should be connected in a synchronous mode and evaluated. More rigorous penetration and depth capability tests should also be made to determine the precise capabilities of the instrument.

Further reduction in size and weight is definitely possible, particularly in the receiver where ordinary nonminiature controls and a relatively large case are now in use. Printed circuit techniques might be applied to the loop assemblies to increase the dimensional stability while trimming weight and assembly costs.

The phase sensitivities of a single parallel RLC circuit near resonance are given by

$$\frac{\partial\phi}{\partial L} = \frac{Q}{L} \quad (10)$$

$$\frac{\partial\phi}{\partial C} = \frac{Q}{C} \quad (11)$$

and

$$\frac{\partial\phi}{\partial f} = \frac{2Q}{f} \quad (12)$$

Phase adjustment is available over a wide range using both the transmitting and receiving loop trimming capacitors. The receiving loop trimmer must be set to within ± 20 picofarads to establish a phase reference within ± 6 degrees of that desired. As this corresponds to a ± 20 degree rotation of a screwdriver adjustable control, it would appear that a front panel knob-variable 75 picofarad capacitor would provide a more precise adjustment and allow compensation for instrument height and ground conductivity. A dual or Butterfly type of capacitor would be required.

The total phase sensitivity of the synchronous system to a frequency shift Δf is given by

$$\frac{\Delta\phi}{\Delta f} = \frac{2}{f} \sum_1^r Q_n \quad (13)$$

where Q_n is the Q of each cascaded but isolated parallel RLC circuit near resonance. For the model locator $\sum Q_n = 15 + 30 + 8 + 8 + 4 = 65$. For a short term phase stability of 0.6 degrees, the transmitter frequency must remain within 6 parts in 10^5 of its initial value, a figure well within the capabilities of the present oscillator.

The high phase sensitivity to changes in system frequency strongly suggests that feedback be employed to form a quadrature null-seeking loop which would serve to hold the detection system at maximum sensitivity while providing automatic compensation for varying values of ground conductivity and instrument height. This would force the locator to be at a point of optimum detectability at all times.

Target discrimination would be achieved by placing a relatively long integration time on the AFC loop, perhaps on the order of four to five seconds. As only a fraction of a second is required to traverse the edge of a target, a strong output would be produced for sudden changes in conductivity, while gradual changes and system drift would provide their own correction.

The voltage at the base of the expander stage, taken with respect to transmitter ground, is a 0 to 500 millivolt quadrature demodulated DC output signal. This signal could be returned to the transmitter, integrated with a five second RC integrator, and applied to a varactor diode shunting the low-level side of the ceramic resonator. AFC gain would not necessarily be required, owing to the high input impedance of a reverse biased varactor. Preliminary tests have indicated this to be feasible using large varactors, zero bias, and no AFC gain. As only a few additional low cost parts would be required for an instrument of superior detectability, the inclusion of such an AFC loop should be an important and immediate area for further study.

CONCLUSIONS

Because the receiver-transmitter type of electronic metal locator does not possess a sixth order response dropoff for depths comparable to the instrument's length, it represents the best choice of currently available metal locator designs when depth of penetration is a primary objective. The operating frequency must represent a compromise between the effects of terrestrial absorption and the inductive coupling sensitivity.

Integrated circuitry techniques lend themselves well to the receiver-transmitter locator, and are of definite value in minimizing field pattern distortion as well as the total weight and cost of such an instrument. Secondary benefits are derived in the form of long battery life, ease of operation, and greatly simplified circuitry in the form of balanced differential amplifier stages.

Nonlinear signal processing is realizable with a relatively simple circuit, and is of value in the evaluation and interpretation of signal returns.

Synchronous demodulation of return signals offers an effective means of separating the in-phase return signal of a metallic target from the quadrature returns caused by straight-through coupling and dielectric ground reflection, but is applicable to the receiver-transmitter system only if a totally balanced receiver, transmitter, and synchronous demodulator are used. Unbalance of any sort results in pattern distortions that adversely affect detection and lead to ambiguous target indications.

A permanently synchronous system is undesirable as it prevents several detector functions that require the separation of receiver and transmitter.

Adding a slow AFC integral feedback path to serve as a quadrature phase lock loop should render the detector relatively immune to straight-through and ground return clutter, automatically correcting the instrument's drift and holding to parameters of optimum detectability.

BIBLIOGRAPHY

1. Lancaster, Donald E., Electronic Metal Locators, to be published in ELECTRONICS WORLD.
2. Krauss, John D., Antennas, McGraw-Hill, New York, 1950, p. 7.
3. Jasik, Henry, Antenna Engineering Handbook, McGraw-Hill, New York, 1961, pp 2-4.
4. Schafer, Curtiss R., Industrial Metal Detector Design, ELECTRONICS, November 1951, pp 86-91.
5. Grover, Frederick W., Inductance Calculations, D. Van Nostrand Co., New York, 1946, Chapter 11.
6. Heiland, C. A., Geophysical Exploration, Prentice Hall, Inc., Englewood Cliffs, N. J., 1946, Chapter 10.
7. Op. Cit., Reference 4.
8. Department of the Army Technical Manual TM5-9541, AN PRS 4 Detecting Set, Mine, Balanced UHF System Type, September 1953, Section 63:90.
9. Garner, Louis E., Some Interesting SONALERT Applications, Electropac, Inc., Peterborough, N. H., August 1964.
10. Lancaster, Donald E., Using the New Low Cost Integrated Circuits, ELECTRONICS WORLD, March 1965, pp 50-52.
11. Lancaster, Donald E., Understanding the Differential Amplifier, to be published in ELECTRONICS WORLD.
12. Robertson, J. J. and Hirschfield, R. A., Application of Micro-Electronics to IF Amplifiers, Application Note AN-160, Motorola, Inc., Phoenix, Arizona.

13. Department of the Army Technical Manual TM 11-1122, SCR625A Detector, Anti Tank Mine, Portable M1, 1943.
14. Curtis, Leslie F., Detectors for Buried Metallic Bodies, National Electronics Conference Proceedings, Chicago, Illinois, 1946, p 339.
15. Clapp, C. W., Detecting Tramp Metal in Logs and Iron Ore, ELECTRONICS, March 1951, pp 89-93.

BIOGRAPHICAL SKETCH

Donald E. Lancaster was born on January 13, 1940 and received the BSEE degree from Lafayette College in 1961. He has done graduate study at Carnegie Institute of Technology before pursuing the MSEE degree at Arizona State University.

Mr. Lancaster is presently a circuit design engineer with the Goodyear Aerospace Corporation and specializes in the fields of solid state circuitry and radar system analysis. He has a patent and has written over 125 technical articles to date, which have appeared in the major electronics trade journals. He is married and a member of the IEEE.